Stochastic Signal Processing and Transduction in Chemotactic Response of Eukaryotic Cells

Masahiro Ueda* and Tatsuo Shibata†
*Laboratories for Nanobiology, Graduate School of Frontier Biosciences, Osaka University, Suita, Osaka, Japan; and †Department of Mathematical and Life Sciences, University of Hiroshima, Higashi-Hiroshima, Hiroshima, Japan

ABSTRACT Single-molecule imaging analysis of chemotactic response in eukaryotic cells has revealed a stochastic nature in the input signals and the signal transduction processes. This leads to a fundamental question about the signaling processes: how does the signaling system operate under stochastic fluctuations or noise? Here, we report a stochastic model of chemotactic signaling in which noise and signal propagation along the transmembrane signaling pathway by chemoattractant receptors can be analyzed quantitatively. The results obtained from this analysis reveal that the second-messenger-production reactions by the receptors generate noisy signals that contain intrinsic noise inherently generated at this reaction and extrinsic noise propagated from the ligand-receptor binding. Such intrinsic and extrinsic noise limits the directional sensing ability of chemotactic cells, which may explain the dependence of chemotactic accuracy on chemical gradients that has been observed experimentally. Our analysis also reveals regulatory mechanisms for signal improvement in the stochastically operating signaling system by analyzing how the SNR of chemotactic signals can be improved on or deteriorated by the stochastic properties of receptors and second-messenger molecules. Theoretical consideration of noisy signal transduction by chemotactic signaling systems can further be applied to signaling systems in general.

INTRODUCTION

Living cells can sense and respond to environmental signals through dynamic signaling processes in the reaction networks of biomolecules. Because biomolecules operate stochastically under the strong influence of thermal fluctuations, living cells can be referred to as stochastically operating biomolecular computation systems. Recent progress in the area of single-molecule detection techniques has identified the stochastic nature of biomolecules in vitro and in living cells (1,2). For example, single ion channels have been observed to exhibit a random transition between open (''on'') and closed (''off'') states in an alternating manner (3). Such stochastic behavior has also been observed in catalytic reactions by single enzyme molecules and in steplike movements by single molecular motors (4–7). On-off fluctuations in individual molecules inevitably cause number fluctuations in the ensemble of the molecules, thus making intracellular signaling processes inherently noisy. This leads to a fundamental question about intracellular signaling processes in general: how does the signaling system operate reliably under thermal and stochastic fluctuations? To gain insight into how signals are received, processed, and transduced by stochastically operating molecules, we study the chemotactic signaling system of eukaryotic cells as a typical example of a stochastic computation system.

Chemotaxis is a fascinating phenomenon in which cells sense chemical gradients and move with directional preference toward or away from the source of the chemical cues. Eukaryotic cells can sense the differences in chemoattractant concentration across the cell body and respond by extending pseudopods directed up the chemical gradient (8–12). In *Dictyostelium* cells, extracellular cyclic adenosine 3′, 5′-monophosphate (cAMP) functions as a chemoattractant. Only 2% gradients can induce a biased movement of the cells toward the source of cAMP in a wide range from 10 pM to ~10 μM (13–15). Because *Dictyostelium* cells are 10–20 μm in size and contain ~80,000 receptors on the surface evenly, with an average K_d of ~100 nM (16,17), receptor occupancy is estimated to be ~16,000 molecules at the maximum efficiency of chemotaxis (25 nM), whereas the differences in receptor occupancy between the anterior and posterior halves are ~130 with 2% gradients. Recently, the lowest gradient value where directed motion is observed was determined by using microfluidic devices (18). The difference in receptor occupancy was estimated to be only on the order of 10 molecules for gradients close to the lower threshold (~10^{-3} nM/μm). Ligand binding to the receptors is a stochastic process, so receptor occupancy should fluctuate with time and space. Assuming a Poisson process, fluctuations in receptor occupancy are the square root of the averaged occupancy, and therefore ~130, which is comparable to the spatial differences. Around the threshold stimulation (100 pM), occupancy and its fluctuations are ~80 ± 9 molecules, whereas the differences are ~1 to ~8 molecules with 2% to ~20% gradients. Although this estimation includes many uncertainties, it implies that the input signals for chemotaxis become noisy due to the fluctuations in ligand

Submitted November 1, 2006, and accepted for publication February 15, 2007.

Address reprint requests to Masahiro Ueda, Laboratories for Nanobiology, Graduate School of Frontier Biosciences, Osaka University, Yamadaoka 1-3, Suita, Osaka 565-0871, Japan. Tel.: 81-6-6879-4632; Fax: 81-6-6879-4634; E-mail: ueda@phys1.med.osaka-u.ac.jp.

Editor: Thomas Schmidt.

0006-3495/07/07/11/10 $2.00

doi: 10.1529/biophysj.106.100263

binding to the receptors. Such fluctuations in signal input have been observed directly by single-molecule imaging of the attractant bound to living *Dictyostelium* cells (19). Chemotactic signaling systems should amplify small changes in input signals. However, by the same system, small random changes (noise) in the input signal would be amplified also, resulting in the propagation of noise as well as signal. Thus, how chemotactic cells reliably obtain information regarding the gradient from such noisy input is a critical question for directional sensing in chemotaxis.

Stochastic signaling processes in living cells have been studied theoretically. Oosawa constructed a theory of spontaneous signal generation in living cells based on thermal fluctuations of biomolecules (20–22). Berg and Purcell have shown that chemoreception by receptors is limited by molecular counting noise (23). For the chemotaxis of amoeboid cells, Tranquillo and colleagues constructed a stochastic model in which the ligand-receptor binding reaction generates stochastically the intracellular messenger that is the critical regulator of the motile system to modulate turning frequency of cells. Based on kinetic fluctuations in ligand-receptor binding, the model explains well the characteristic features of leukocyte random motility and chemotaxis (24,25). Recently, generation and propagation of noise in intracellular processes have been studied in engineered transcriptional regulatory networks (26–29). Elowitz and colleagues have clearly shown experimentally that noise propagates along a cascade of gene expression. Paulsson unified the gene network experiments by analyzing the propagation of noise in gene networks from a theoretical point of view (30). Shibata and Fujimoto addressed how noise relates to the amplification of signals in intracellular signaling processes, which is summarized as the gain-fluctuation relation (31). The relation tells us that signal and noise propagation along the signaling cascade can be characterized by the gain and characteristic time of the signaling reactions, which can be applied generally to intracellular signaling reactions including Michaelis-Menten, allosteric, and push-pull reactions. Recent progress in imaging techniques to monitor directly intracellular signaling reactions makes it possible to determine stochastic properties of signaling molecules, and therefore a theoretical framework is required to evaluate quantitatively how the properties of signaling molecules affect cellular response.

Here we consider a simple but general model in which receptors receive ligands stochastically and the resulting active receptors generate second messengers stochastically. We applied the gain-fluctuation relation to this model, by which the signal/noise ratio (SNR) of chemotactic signals can be calculated based on the properties of the signaling molecules obtained experimentally. Analysis of the SNR reveals that directional sensing in eukaryotic chemotaxis is limited by receptor-generated stochastic noise, and also reveals how the stochastic nature of the receptor and second messengers affects the SNR of chemotactic signals, which suggests regulatory mechanisms for the noisy signal transduction in chemotactic cells. Our model provides a theoretical framework with experimental approaches to the chemotactic signaling system and can further be applied to stochastic signaling systems in general.

RESULTS AND DISCUSSION

Noisy signal inputs and propagation for chemotaxis in *Dictyostelium* cells

Single-molecule imaging of ligand binding to chemoattractant receptors in living *Dictyostelium* cells demonstrates that signal inputs fluctuate with time and space (Fig. 1 *A*)(19,32). The lifetime of ligand binding shows an exponential distribution, with time constants ranging between ~1 and ~3 s (Fig. 1 *B*). The time series of receptor occupancy exhibits fluctuations (Fig. 1 *C*) with exponential time correlations. These results demonstrate that ligand binding can be described basically as a Poisson process. This means that the chemotactic ligand binds to the receptor randomly and, hence, that input signals are noisy. Note that such fluctuations in input signal are not derived from an error of experimental measurements. The fluctuations are due to the stochastic nature of the ligand-binding process, which is accompanied inherently by the ligand-binding reaction.

We have developed a stochastic model that describes the signal and noise propagation along the transmembrane signaling pathway by receptors. As shown in Fig. 2 *A*, we assume that receptors receive ligands randomly as signal input, leading to the stochastic generation of intracellular messengers as output. The second output messengers then degrade with time. This scheme is representative of many signaling pathways. In the chemotactic signaling system of *Dictyostelium* cells, the first and subsequent reactions correspond to cAMP binding to the receptor and G-protein activation, respectively (10–12). The noise of the active receptors is the deviation from the average amount of active receptors, which can be quantified by $\sigma_{\mathrm{R}}^2 = (R^* - \overline{R^*})^2$, where R^* is the molecular number of active receptors per cell and $\overline{R^*}$ is its average. Assuming that the receptors distribute uniformly on the surface of the cells, the noise, σ_{R}^2, is given by the gain-fluctuation relation (31), as follows,

$$\frac{\sigma_{\mathrm{R}}^2}{\overline{R^*}^2} = g_{\mathrm{R}} \frac{1}{\overline{R^*}}, \tag{1}$$

where the gain, g_{R}, quantifies the response of receptors, ΔR^*, to small changes in ligand concentration, ΔL, which is defined as

$$g_{\mathrm{R}} = \frac{\Delta \overline{R^*}/\overline{R^*}}{\Delta L/L} = \frac{\partial \log \overline{R^*}}{\partial \log L}. \tag{2}$$

From Eq. 2, it is clear that a reaction with higher gain is more sensitive to small changes in input signal, resulting in

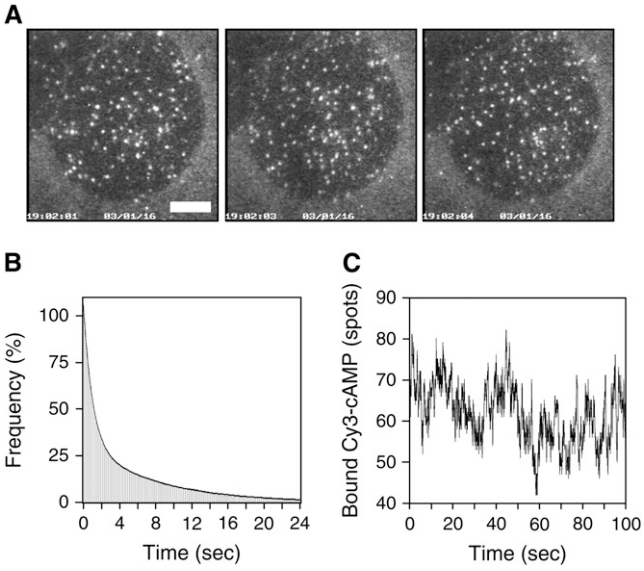

FIGURE 1 Fluctuations in signal inputs for chemotactic response. (*A*) Single-molecule imaging of a fluorescent-labeled cAMP (Cy3-cAMP) bound to the receptor in living *Dictyostelium* cells. Cy3-cAMP was added uniformly to *Dictyostelium* cells at 10 nM. The basal surface of the cells was observed by using total internal reflection fluorescence microscopy, as described previously (19,32). Individual white spots are single molecules of Cy3-cAMP bound to the receptors in living cells. Time, h:min:s. Scale bar, 5 μm. (*B*) Cumulative frequency histogram of lifetime of Cy3-cAMP spots. The lifetimes of individual Cy3-cAMP molecules were obtained by counting the time duration between the appearance and disappearance of the fluorescent spots. The line represents the fitting of data to a sum of two exponential functions, $f(t) = a_1\exp[-k_1t]+a_2\exp[-k_2t]$, where a_1, a_2, k_1, and k_2 are fitting parameters. k_1 and k_2 are dissociation rates, the inverse of the average lifetime. The number of Cy3-cAMP spots analyzed was 1024. $k_1 = 1.0$ and $k_2 = 0.13\ s^{-1}$. $a_1 = 74.3\%$ and $a_2 = 31.4\%$. (*C*) Time course of the number of Cy3-cAMP spots bound to the basal surface of the cells, showing the number fluctuations of signal inputs for chemotactic response.

higher amplification of the signals. However, Eq. 1 tells us that the reaction with higher gain also generates larger noise, because noise is proportional to g_R. That is, a higher gain is required for higher amplification of input signals, but it also inevitably and simultaneously increases noise. When the ligand-binding reaction is described by $R+L \leftrightarrow R^*$, the gain, g_R, decreases as the increase of ligand concentration, L (Fig. 3 *A*; see Eq. 9), and, hence, the relative noise, $\sigma_R/\overline{R^*}$, decreases (Fig. 3 *C*). Thus, chemotactic cells receive noisier signals at lower ligand concentrations.

The active receptor, R^*, leads to the stochastic activation of intracellular messenger X to the active form X^* as output. The noise of the active second-messenger concentration σ_X^2 is described by (30,31)

$$\frac{\sigma_X^2}{\overline{X^*}^2} = g_X\frac{1}{\overline{X^*}} + g_X^2\frac{\tau_R}{\tau_X+\tau_R}\frac{\sigma_R^2}{\overline{R^*}^2}, \quad (3)$$

where $\overline{X^*}$ and g_X are, respectively, the average number of active second messengers and the gain of the reaction, defined as $g_X = (\Delta\overline{X^*}/\overline{X^*})\times(\Delta R^*/R^*)^{-1}$. τ_R and τ_X are the characteristic time constants of the ligand-binding reaction and second-messenger-production reaction, respectively, which are defined by the rate constants of the corresponding reactions (see Eq. 10).

The second term on the righthand side of Eq. 3 is the extrinsic noise (26), which describes how the noise of active receptor R^* propagates into the noise of second-messenger concentration. When the time constant of the second-messenger production is faster than that of the active receptor ($\tau_X \ll \tau_R$), the noise of the active receptor is propagated more efficiently into the noise of the second messenger, with a decrease in τ_X, because the term $\tau_R/(\tau_X+\tau_R)$ increases gradually and reaches unity as τ_R/τ_X increases. In this case, the second-messenger-production reaction can follow rapid temporal changes of the active receptor. On the other hand, in the case of $\tau_X \gg \tau_R$, the second-messenger reaction cannot follow the noise of the active receptor. Instead, the noise of the active receptor is averaged temporally, and the extrinsic noise decreases. In the extreme case, the extrinsic noise is eliminated from the total noise by time-averaging effects. Thus, the relatively slower reaction is required in the second-messenger production to reduce the extrinsic noise generated by the ligand-binding reaction, whereas the relatively faster reaction causes the noise propagation.

Even if the amount of active receptor is constant without noise ($\sigma_R = 0$) or the extrinsic noise is almost neglected by the effect of temporal averaging in the second-messenger reaction, the second messenger should be accompanied by noise, because the active receptors activate stochastically the second messenger. Such intrinsically generated noise by the second-messenger-activation reaction itself is called intrinsic noise (26), which is given by the first term on the righthand side of Eq. 3. The intrinsic noise is included inevitably in the total noise of second messengers. Fig. 3 *D* shows the relative contributions of intrinsic and extrinsic noise to the total noise. The total noise, $\sigma_X/\overline{X^*}$, increases with decreasing ligand concentration. Because extrinsic noise is proportional to the square of the gain, whereas intrinsic noise is proportional to the gain (Eq. 3), extrinsic noise contributes dominantly to the total noise in the lower ligand-concentration ranges, where the gain, g_X, becomes relatively higher (Fig. 3 *B*). On the other hand, intrinsic noise contributes dominantly in the higher ligand-concentration ranges (Fig. 3 *D*, *inset*). Thus, the receptors generate noisier signals in the lower ligand-concentration range, which would take into account the inefficient chemotaxis in the corresponding ranges, as described in the next section.

Limitation of directional sensing by noise

To explain the mechanisms whereby cells sense chemical gradients, two representative mechanisms have been proposed: temporal sensing and spatial sensing mechanisms (8,9,23,33). In the temporal sensing mechanism, the movements of cells or their parts, such as pseudopods, are

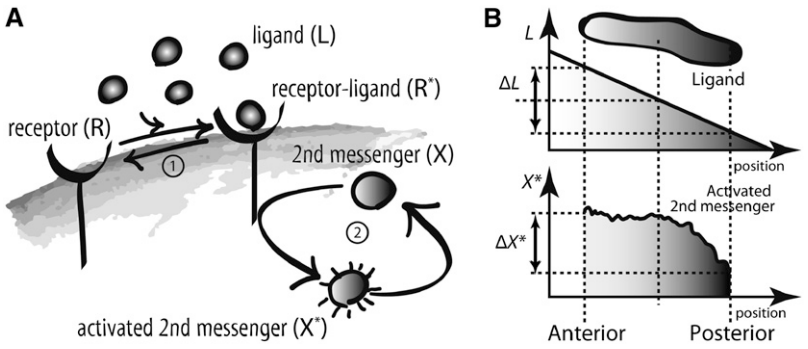

FIGURE 2 Stochastic model of chemotactic signaling. (*A*) Signal transduction reactions by chemoattractant receptors. The ligand (L) binds to the inactive receptor (R), leading to the formation of an active receptor (R^*), which produces the active second messenger (X^*) from the inactive precursor (X). The active X^* is switched off to the inactive state, X, in due time. These reactions can be described by Michaelis-Menten kinetics. (*B*) The cell is placed under a ligand-concentraion gradient. L, average concentration; ΔL, difference in ligand concentration between the anterior and posterior ends of the cell. The anterior and posterior halves sense $\overline{L}+(\overline{\Delta L}/4)$ and $\overline{L}-(\overline{\Delta L}/4)$ on average, respectively. The difference in receptor occupancy ΔR^* is produced from ligand-concentration differences, which lead to the difference in second messenger, ΔX^*, between the anterior and posterior halves. The differences ΔR^* and ΔX^* should include the noise $\sigma^2_{\Delta R}$ and $\sigma^2_{\Delta X}$ around average values $\overline{\Delta R^*}$ and $\overline{\Delta X^*}$, respectively.

essential for gradient sensing, in which the spatial differences in chemoattractant concentration are converted into temporal changes through the movements. In the spatial sensing mechanism, cells detect the signals simultaneously at different points over their surfaces. As a result of comparison of the detected signals, the cells sense the direction of the chemical gradient. *Dictyostelium* cells can form positive or negative gradients of some signaling molecules, such as PI3-kinase and PTEN (tensin homology protein), inside the cell along the gradient of cAMP without cell movements and pseudopod extensions, indicating that the cells can sense the higher-concentration side of cAMP across the cell body without motion, which provides strong evidence that the origin of chemotactic signals is spatial differences in receptor occupancy (10–12). Thus, the cells do not necessarily require temporal sensing mechanisms for gradient sensing.

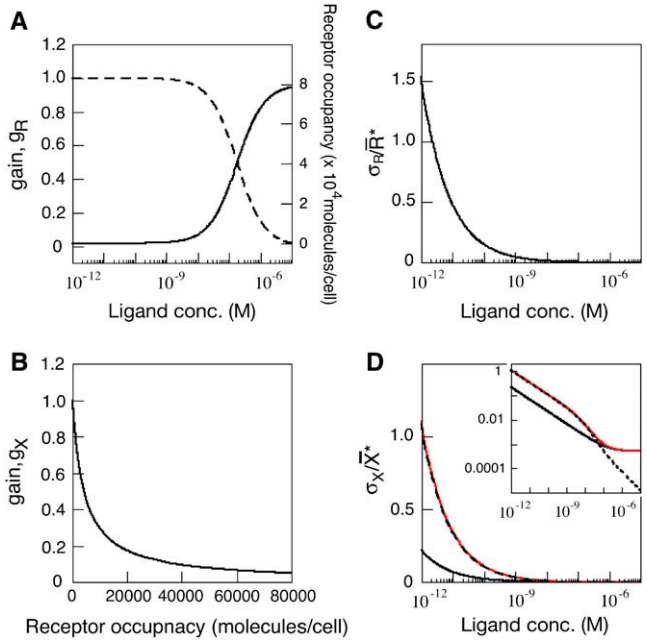

FIGURE 3 Relationship between gain and noise. (*A*) Active receptor concentration (R^*; *solid line*) and gain (g_R; *dashed line*) plotted as functions of ligand concentration. (*B*) Dependence of the gain g_X on receptor occupancy. (*C*) Dependence of relative noise in R^* on ligand concentration. (*D*) Dependence of relative noise in X^* on ligand concentration. Extrinsic noise and intrinsic noise are represented by black dashed and solid lines, respectively. The total noise strength is represented by the red solid line. The parameter values used for the calculation are summarized in Table 1. (*Inset*) Log-log plot. Extrinsic noise contributes dominantly to the total noise in the lower ligand-concentration range, whereas intrinsic noise contributes dominantly in the higher ligand-concentration ranges.

Devreotes and colleagues propose an alternative mechanism, the so-called local excitation global inhibition (LEGI) mechanism, in which temporal and spatial mechanisms are integrated to take into account the behavior of chemotactic cells (10,34,35). In the LEGI mechanism, receptor occupancy in a local area determines the local level of excitation, whereas the average level of receptor occupancy over the entire surface of the cell determines the level of inhibition in all regions of the cell. Although this mechanism does not assume direct comparison of the ligand concentration between different points over the cell surface, spatial differences of the ligand concentration are sensed through a comparison between the excitatory signals and the inhibitory signals at each of the local areas. Thus, chemotactic signals in the LEGI mechanism are derived from differences in receptor occupancy between the local region and the total surface of the cells. With regard to the origin of chemotactic signals, the LEGI mechanism can be thought of as an extension of the spatial sensing mechanism, which provides the molecular basis for the comparison of the spatial differences in receptor occupancy across the cell body. Although the temporal sensing mechanism may have a role for gradient sensing of chemotactic cells, the spatial sensing mechanism is essential, as described above. Here, we discuss the signal and noise propagation based on the spatial sensing mechanism, in which the chemotactic signals are the spatial differences in receptor occupancy across

the cell body. We did not consider sensory adaptation in our model, because G-protein activation does not exhibit adaptation in *Dictyostelium* cells when ligand stimulation is applied continuously to cells (36).

We consider the differences in second-messenger concentration, ΔX^*, between the higher- (anterior) and lower (posterior)-ligand-concentration regions of chemotactic cells placed under a chemical gradient. As shown in Fig. 2 *B*, the concentration difference in the ligand concentration, ΔL, may produce the difference in receptor occupancy, ΔR^*, which may then lead to the difference in second-messenger concentration, ΔX^*, between the anterior and posterior regions of chemotactic cells. The ΔR^* and ΔX^* should include the noise, $\sigma^2_{\Delta R}$ and $\sigma^2_{\Delta X}$ around the average values, $\overline{\Delta R^*}$ and $\overline{\Delta X^*}$, respectively.

To evaluate the effects of the noise on gradient sensing, we studied the SNR, defined as $\overline{\Delta X^*}/\sigma_{\Delta X}$. From Eq. 3, we obtain the following relation between $\sigma_{\Delta R}/\overline{\Delta R^*}$ and $\sigma_{\Delta X}/\overline{\Delta X^*}$ (see Appendix for derivation).

$$\frac{\sigma^2_{\Delta X}}{\overline{\Delta X^*}^2} = \frac{1}{g_X \overline{X^*}}\left(\frac{\overline{R^*}}{\overline{\Delta R^*}}\right)^2 + \frac{\tau_R}{\tau_X + \tau_R}\left(\frac{\sigma_{\Delta R}}{\overline{\Delta R^*}}\right)^2, \qquad (4)$$

where the first and second terms on the righthand side are the intrinsic and extrinsic noise, respectively, of gradient sensing. The SNR, $\overline{\Delta X^*}/\sigma_{\Delta X}$, is obtained by the inverse of the square root of Eq. 4.

Fig. 4 *A* shows dependence of the SNR, $\overline{\Delta X^*}/\sigma_{\Delta X}$, on the average concentration of ligand. The parameter values to calculate the SNR for *Dictyostelium* cells are summarized in Table 1 (see Appendix and Eq. 11). We also performed stochastic numerical simulation showing agreement with our theory (Fig. 4 *A*). The SNR of chemotactic signals attains a maximum at the ligand concentration between the affinity of the receptor, K_d, and the EC_{50} concentration, where the G-protein activation reaches half-maximum. This optimal concentration value is dependent mainly on the receptor affinity K_d, and is relatively unaffected by the EC_{50} variation of G-protein activation (data not shown). In the lower-ligand-concentration range, the SNR is determined mainly by the contribution of the extrinsic noise, meaning that the fluctuations in active receptor dominantly affect the quality of the chemotactic signals. In the higher-ligand-concentration range, the SNR deteriorates with an increase in ligand concentration, because receptors are gradually saturated, making them unable to produce the large differences in second-messenger concentration between the anterior and posterior halves of cells, leading to an increase in intrinsic noise.

We next examined the relationship between the SNR of chemotactic signals and the signaling accuracy. As shown in Fig. 4 *C*, the time series of ΔX^* obtained by numerical calculation indicates that ΔX^* can sometimes be negative. This means that the concentration gradients of second messengers can be reversed against ligand-concentration gradients by fluctuations in ligand binding and second-messenger

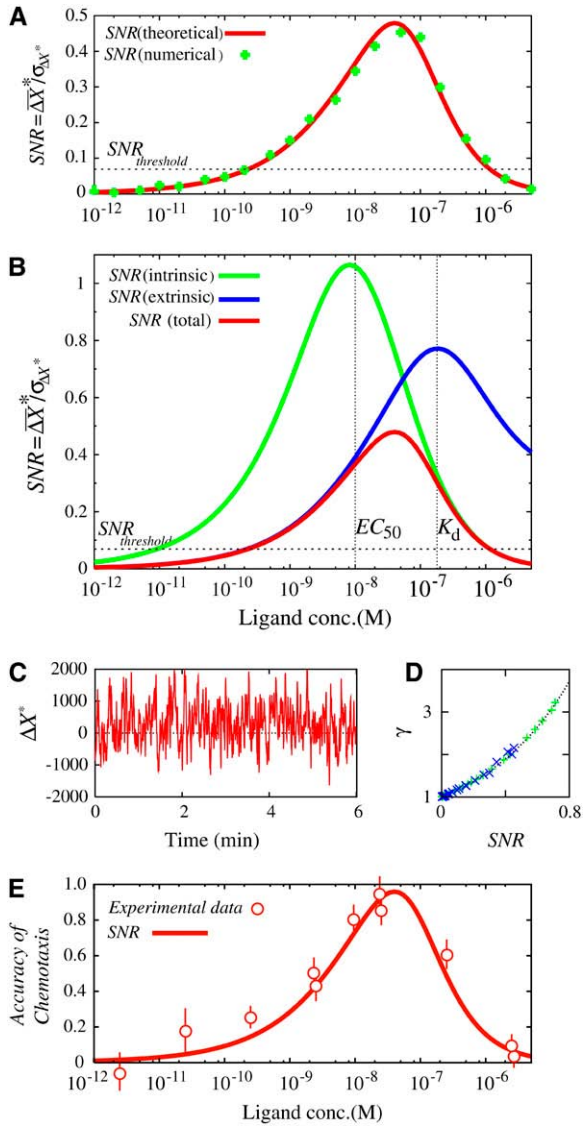

FIGURE 4 SNR of chemotactic signals. (*A*) Dependence of the SNR on ligand concentation obtained theoretically by Eq. 4 (*red line*) and numerically (*green diamonds*). The cell is located without locomotion under a linear chemoattractant gradient of 2% along the anterior-posterior axis with the midpoint concentration *L*. The parameter values used for the calculation are summarized in Table 1. For the simulation, the spatial coordinate of the cell is discretized into small boxes appropriately, and the reactions take place in each box according to the Gillespie's algorithm (44). (*B*) Relative contributions of extrinsic (*blue*) and intrinsic (*green*) noises on the total SNR of chemotactic signals (*red*). (*C*) Numerical calculation of chemotactic signals. Time course of second-messenger concentration difference (ΔX^*) between anterior and posterior halves of single cells. $L = 0.01$ μM. (*D*) A proportional relation between the SNR of chemotactic signals and γ, which represents the ratio between the total time durations with $\Delta X^* > 0$ and $\Delta X^* < 0$. *Dashed line*, $(1 - \mathrm{Erf}(-SNR/\sqrt{2}))/\ (1 - \mathrm{Erf}(SNR/\sqrt{2}))$, where Erf($x$) is the error function. (*E*) Comparison of the SNR with Fisher's experimental data for chemotactic accuracy of *Dictyostelium* cells (14). The SNR obtained theoretically (*red line*) was overlaid on the experimental data (*red circles*). (Adapted from Fig. 5 of Fisher et al. (14) with permission). The SNR was plotted on the same scale as in *A*.

TABLE 1 Model parameters

	Parameters	Values
Φ	Cell length	10 μm
ΔL	Gradient	$0.02L^*$
R_{total}	Total receptor	80,000 molecules/cell†
K_R	Ligand affinity	0.18 μM†
k_{off}	Dissociation rate	1 s^{-1}†
k_{on}	Association rate	5.6 s^{-1} μM^{-1}†
X_{total}	Total second messenger	200,000 molecules/cell‡
EC_{50}	§	0.01 μM§
K_X	§	4210 molecules/cell§
k_d	X degradation rate	1.0 s^{-1}‡
k_p	X production rate	1/4210 s^{-1}(molecules/cell)$^{-1}$¶

X represents G-protein, because the second reaction is G-protein activation in *Dictyostelium* cells.

*The gradient is expressed as the concentration difference between the anterior and posterior ends of a cell. For calculation of the SNR, the concentration difference at the center of anterior and posterior regions was used, and the difference, ΔL, is $0.01L$ (13,14).

†Receptor number, ligand affinity, and dissociation rate were obtained experimentally (Fig. 1) (16,17,19). Association rate was obtained from K_R and k_{off}.

‡The values were inferred.

§EC_{50} and K_X are the concentration of cAMP and active receptor where the activation of the second messenger reaches half-maximum, respectively (36). K_X was obtained from EC_{50}, K_R, and R_{total}, according to Eq. 8.

¶k_p was determined by $k_p = k_d/K_x$.

production reactions. Because chemotaxis is expected to be more accurate when $\Delta X^* > 0$ is produced more frequently, the ratio between the total time durations with $\Delta X^* > 0$ and $\Delta X^* < 0$, γ, can be used as an index of chemotactic signaling accuracy. As shown in Fig. 4 *D*, the ratio γ increases in proportion to the SNR. Thus, when chemotactic signals have a higher SNR, ligand gradients are represented on the second-messenger gradient for a longer time, which would lead cells to exhibit chemotaxis more accurately.

The chemotactic accuracy of *Dictyostelium* cells has been measured experimentally by Fisher et al. (14). The dependence of chemotactic accuracy on ligand concentration exhibits a profile similar to our calculated SNR (Fig. 4, *A* and *E*). In the experiment, the cell's movements were biased toward the higher concentration of cAMP over a range of 10 pM to 10 μM, and chemotactic accuracy attained a maximum at 25 nM of cAMP concentration. This optimal value is almost the same as the concentration at which the SNR reaches the maximum (Fig. 4 *E*). The agreement between the SNR and chemotactic accuracy indicates that the ability of directional sensing is limited by the inherently generated stochastic noise during the transmembrane signaling of receptors. Note that Eq. 4 does not depend on a particular detail of the spatial sensing mechanism, and can be applied to other systems. In fact, similar dependence of chemotactic accuracy has been observed in mammalian leukocytes and neurons, although these cells exhibit chemotaxis at different ranges of ligand concentration (37,38). Such differences in the dependence of chemotactic accuracy on ligand concentration can be explained by cell-type-specific parameters, such as the ligand-binding affinity of receptor, K_d, and the EC_{50} concentration for second-messenger activation.

When the ligand concentration L is sufficiently small ($L \ll K_R$, K_{XR} in Eq. 11), the SNR of the chemotactic signals changes in a manner of $SNR \propto \Delta L/\sqrt{L}$. If the cell requires a signal exceeding a threshold SNR to detect chemical gradients, the cell will exhibit a threshold, $\Delta L_{threshold}$, for each ligand concentration L for chemotaxis. Then, supposing that such threshold SNR is independent of ligand concentration L, we obtain the relation $\Delta L_{threshold} \propto L^{0.5}$. The threshold gradient in a given concentration of ligands can be measured experimentally. In fact, Van Haastert (39) reported the relation between the average concentration of ligand and the corresponding threshold gradient at which 50% of the cells can respond in the chemotactic assay. He found that α for $\Delta L_{threshold} \propto L^{\alpha}$ was estimated to be 0.35, which largely agrees with our estimation. In the experiments, the relatively high background cAMP concentrations were used to reveal sensory adaptation processes. Then, the threshold relation is not simply applicable at experimental conditions. Sensory adaptation, which was not considered in our model, may contribute to the α value being lower than theoretical estimation. To further evaluate our model, similar experiments would be required at the lower background concentrations in shallow gradients.

According to Eq. 11, the SNR changes in proportion to ΔL at a given concentration of ligands, L. Fisher et al. also studied the dependence of chemotactic accuracy on ΔL at 25 nM cAMP (14). The accuracy was reduced almost linearly with a decrease of ΔL, vanishing at 10 pM/μm, which was a 0.3% to ~0.6% gradient. From our formula, the SNR for the 0.3% gradient around 25 nM was estimated to be ~0.07. Supposing that such a minimum SNR is a threshold for chemotaxis at any chemoattractant concentration, the ligand concentration required for chemotaxis at 2% gradient ranges from ~200 pM to 1 μM (Fig. 4, *A* and *E*), which is narrower than the observed range of chemotaxis in experiments. Those mechanisms not considered in our model, such as the temporal sensing mechanism or sensory adaptation, may contribute to chemotaxis at the lowest and highest concentration ranges. The role of adaptation in the SNR of chemotactic signals will be discussed elsewhere.

Despite the qualitative agreement between the SNR of chemotactic signals at the receptor level and chemotactic accuracy, the quantitative relationship between the two remains to be clarified. The chemotactic signaling system of *Dictyostelium* cells and other cell types has many components between the receptors and motile apparatus to convert the signals from receptors into unidirectional cell movement. Devreotes and colleagues have revealed that one of the key reactions in the chemotactic signaling system is a distinctive localization of phosphatidylinositol 3,4,5-trisphosphates ($PI(3,4,5)P_3$) on the membrane facing a higher concentration of cAMP (10–12). The $PI(3,4,5)P_3$ localization takes place in

an all-or-none manner, meaning that noisy input is processed and transduced to generate a clear signal reflecting the gradient direction of chemoattractants through the cascades upstream of $PI(3,4,5)P_3$. It would be valuable to examine how the SNR of chemotactic signals at the receptor level is reflected in the dynamics of $PI(3,4,5)P_3$ localization.

Improvement of the SNR of chemotactic signals

Our results suggest how the SNR of chemotactic signals is improved by the properties of the receptors and the downstream second messenger. First, the SNR can be improved with a decrease of τ_R, meaning that faster transitions between the ligand-binding (on) state and ligand-unbinding (off) state of the receptors can produce chemotactic signals with higher SNR (Fig. 5 *A*). When ligand concentration is increased, the ligand association rate ($k_{on}L$) to the receptor is accelerated, resulting in a decrease in the time constant, τ_R (Eq. 10). That is, an increase in ligand concentration results in better efficiency of chemotactic signals not only by increasing the average concentration of the active receptor but also by decreasing the characteristic time of fluctuations of the active receptor. Moreover, signal improvements are possible by increasing the on-rate (k_{on}) and/or off-rate (k_{off}). For example, when the potential barrier between the on-state and off-state of the receptor becomes lower, the cycling between the two states is accelerated by the acceleration of the on-rate (k_{on}) and the off-rate (k_{off}) resulting in a decrease in τ_R and, hence, improvement of the SNR of chemotactic signals. Ueda et al. (19) reported polarity in receptor kinetic states along the length of chemotactic cells, which suggests that the SNR is higher at the pseudopod region than at the tail region. Such polarity in the SNR of chemotactic signals may provide a basis for the polarity observed in the response of *Dictyostelium* cells (40).

Second, the SNR can be improved by increasing τ_X. Longer lifetime of the second messenger, which corresponds to slower degradation, causes noise reduction more effectively through time-averaging of the extrinsic noise (Fig. 5 *B*). This means that the regulatory mechanism for the degradation or the inactivation of second messengers has a pivotal role on the signal improvements for chemotaxis. In the case of G-protein, the hydrolysis rates of the bound GTP on the α-subunit and the reassociation rates with the $\beta\gamma$-subunit mostly determine the lifetimes of active G-proteins, and thus affect the SNR of chemotactic signals. This suggests that the GTPase-activating protein, such as regulators of G-protein signaling (RGS), can regulate the quality of the signal by modulating the inactivation rates of G-protein.

Third, an increase in gain g_X can contribute to improved SNR. A high gain that is larger than unity can be obtained for reactions with some cooperativity or ultrasensitivity (31). Eq. 4 can be applied for such reactions. When the cells use cooperative or ultrasensitive reactions for second-messenger activation, chemotactic signals can be improved through reduction of the intrinsic noise.

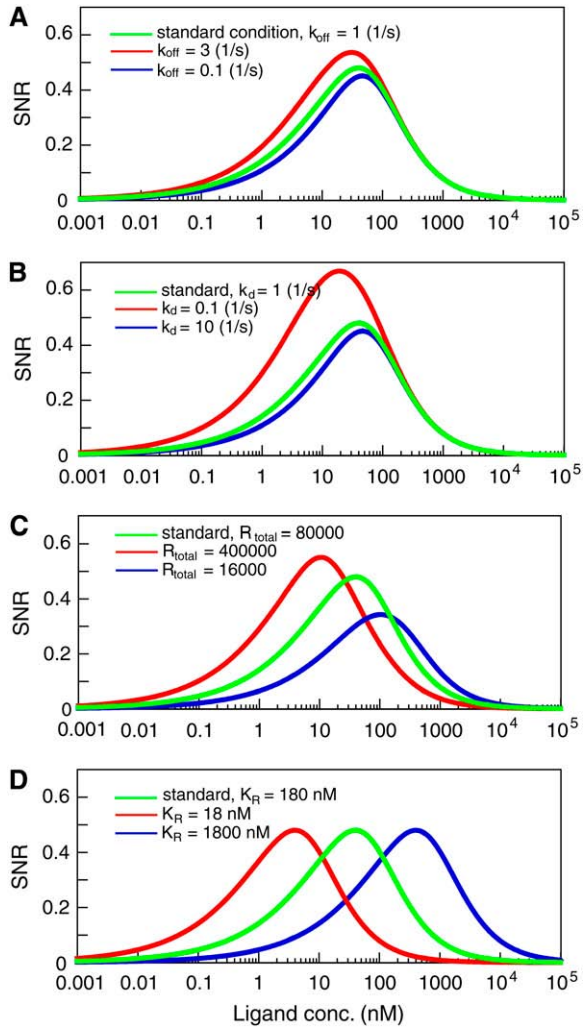

FIGURE 5 Signal improvements. (*A*) Receptor fluctuation-dependent signal improvements. The dissociation rates of a ligand (k_{off}) were changed: (*blue line*) 0.1 s^{-1}; (*green line*) 1 s^{-1} (standard condition); (*red line*) 3 s^{-1}. (*B*) Time-averaging effects. The SNR was improved by increasing the time constants of the second messenger. The degradation rates (k_d) were changed and the corresponding SNR was calculated: (*blue line*) 10 s^{-1}; (*green line*) 1 s^{-1}; (*red line*) 0.1 s^{-1}. (*C*) Dependency of the SNR on the expression levels of receptors. The receptor numbers per single cell are 16,000 (*blue*), 80,000 (*green*), and 400,000 (*red*) molecules/cell. (*D*) Effects of affinity modulation on the SNR. Ligand-binding affinity: 18 nM (*red*), 180 nM (*green*), and 1800 nM (*blue*).

Fourth, the SNR depends on the total amount of receptor expressed in cells (Fig. 5 *C*). The SNR is improved in the lower and higher concentration ranges of chemoattractant by increasing and decreasing receptor number, respectively. Receptor internalization can contribute to SNR improvements in the higher concentration ranges by decreasing membrane-bound receptors. Also, receptor affinity for the chemoattractant is an important factor in adjusting the concentration ranges in chemotaxis (Fig. 5 *D*). Modification

in the affinity causes a shift in the dependence of SNR on chemoattractant concentration, which would be a basis for a wider-range response. It is well known that the cAMP receptors in *Dictyostelium* cells are phosphorylated with cAMP stimulation, leading to a three- to approximately six-fold decrease in ligand-binding affinity (41). According to our formula, such an affinity shift of receptors contributes to an SNR increase in the higher-ligand-concentration range, and thus extends the response range to higher ligand concentrations.

Our discussion on the minimum model of chemotactic signaling cascade can be generalized for a longer cascade including multistep reactions. In such a case, extrinsic noise would be amplified by the gain or reduced by time-averaging effects at each step. The gain depends on the type of reaction (31) and also on the concentration ranges of the reaction (e.g., Fig. 3, *A* and *B*). Time-averaging of the extrinsic noise depends on the time constants of the reaction at each step, which are usually determined by both the production and the degradation rates of the messenger molecules. Intrinsic noise would be added inevitably to the extrinsic noise at each step. When the time constants of the reactions become longer along the signaling cascade, the SNR of chemotactic signals would have a more improved effect at the lower reactions through time-averaging effects. In such a signaling system, the shallow gradient can be detected at downstream reactions of the cascade even if it does not generate effectively a clear signal at upstream reactions, suggesting that the downstream molecules have a pivotal role in the detection of a faint signal. *Dictyostelium* cells treated with a PI3-kinase inhibitor can exhibit chemotaxis, but it is restricted to the higher concentration range (42), suggesting that PI3-kinase and the PTEN system are required for detection of a faint signal in a noisy environment. Similar reasoning can be applied to parallel cascades with different time constants. Thus, our model can evaluate the quality of signals in the chemotactic signaling system, which can be further applied to stochastically operating signaling systems in general. To reveal how signal and noise are propagated in a stochastic signaling system, it is important to determine experimentally the gains and time constants of reactions along the signaling cascade. Noise propagation along longer signaling cascades will be discussed elsewhere.

APPENDIX: DERIVATION OF SNR OF CHEMOTACTIC SIGNALS

We define chemotactic signals as the difference in the concentration of X^*, ΔX^*, between the anterior and posterior halves of chemotactic cells (Fig. 2 *B*). Since we are interested in chemotaxis in a shallow gradient, the difference ΔL is small enough so that we only consider linear terms with respect to the differences. The average differences, $\Delta\overline{R^*}$ and $\Delta\overline{X^*}$, between the anterior and posterior halves are defined as

$$\Delta\overline{R^*} = g_R \frac{\Delta L}{L}\frac{\overline{R^*}}{2}, \quad \Delta\overline{X^*} = g_X \frac{\Delta\overline{R^*}}{\overline{R^*}}\overline{X^*}, \tag{5}$$

where $\overline{R^*}$ and $\overline{X^*}$ are the average numbers of active receptor and the active second messenger, respectively, in the cell. The noise of the differences in active receptor, $\sigma^2_{\Delta R}$, is approximately equal to the summation of the noise in the anterior and posterior regions, given by $\sigma^2_{\Delta R} = \sigma^2_{R\text{-anterior}} + \sigma^2_{R\text{-posterior}} = \sigma^2_{R^*}$, where the subscripts ''anterior'' and ''posterior'' indicate the regions of the cell. From Eq. 1, we find

$$\sigma^2_{\Delta R} = g_R\overline{R^*}. \tag{6}$$

Similarly, the noise of chemotactic signals, $\sigma^2_{\Delta X}$, is approximated by $\sigma^2_{\Delta X} \cong \sigma^2_{X\text{-anterior}} + \sigma^2_{X\text{-posterior}}$. Since the concentration gradient of ligand is so small, we may expect that the gain, g_X, and the formed gradient of the active receptor are almost constant

$$\sigma^2_{\Delta X} = g_X\overline{X^*} + \left(g_X^2\frac{\tau_R}{\tau_X+\tau_R}\right)\sigma^2_{\Delta R}\left(\frac{\overline{X^{*2}}}{\overline{R^{*2}}}\right). \tag{7}$$

From Eqs. 5 and 7, the relative noise strength of chemotactic signals, $\sigma^2_{\Delta X}/\Delta X^{*2}$, is obtained in Eq. 4. The SNR of chemotactic signals is the square root of the inverse of the relative noise strength.

To calculate the parameters in Eq. 4 for *Dictyostelium* cells, we consider the simplest reaction scheme:

$$R + L \underset{k_{off}}{\overset{k_{on}}{\leftrightarrow}} R^*, \quad R^* + X \xrightarrow{k_p} R^* + X^*, \quad X^* \xrightarrow{k_d} X$$

According to this scheme, the average number of active receptor, $\overline{R^*}$, and second messenger, $\overline{X^*}$, are given by Michaelis-Menten kinetics,

$$\overline{R^*} = R_{total}\cdot L\cdot(K_R+L)^{-1}, \quad \overline{X^*} = X_{total}\cdot\overline{R^*}\cdot\left(K_X+\overline{R^*}\right)^{-1}, \tag{8}$$

where R_{total} is the total molecular number of receptors per single cell, $K_R = k_{off}/k_{on}$ the affinity for the ligand with association and dissociation rate constants k_{on} and k_{off}, X_{total} the total molecular number of second messenger per cell, $K_X = k_d/k_p$ the concentration of active receptor where the activation of the second messenger reaches half-maximum with production and degradation rates k_p and k_d of the second messenger. The gains of active receptor to the ligand concentration and the second messenger to the active receptor number are given by

$$g_R = K_R\times(K_R+L)^{-1}, \quad g_X = K_X\times\left(K_X+\overline{R^*}\right)^{-1}. \tag{9}$$

The time constants of the reactions are calculated by

$$\tau_R = (k_{on}L + k_{off})^{-1}, \quad \tau_X = (k_pR^* + k_d)^{-1}. \tag{10}$$

When Eqs. 5, 6, 8, and 9 are substituted into Eq. 4, the SNR is obtained as a function of L and ΔL by

$$SNR = \frac{\overline{\Delta X^*}}{\sigma_{\Delta X}} = \frac{1}{\sqrt{4\left(\frac{L+K_R}{K_R}\right)\left\{\frac{(L+K_{XR})^2}{V_X\cdot K_{XR}} + \frac{\tau_R}{\tau_X+\tau_R}\left(\frac{L+K_R}{R_{total}}\right)\right\}}}\left(\frac{\Delta L}{\sqrt{L}}\right). \tag{11}$$

Here, $K_{XR} = K_X\times K_R\times(R_{total}+K_X)^{-1}$ is the ligand concentration with which the activation of X reaches the half-maximum value, and $V_X = R_{total}\times X_{total}\times(R_{total}+K_X)^{-1}$. According to Eq. 11, the SNR is proportional to $\Delta L/\sqrt{L}$ when ligand concentration is much smaller than K_R and K_{XR}.

Supposing that cells can sense the gradient if the SNR of chemotactic signals is larger than the threshold SNR, $SNR_{\text{threshold}} \leq C(\Delta L/\sqrt{L})$ with constant C, and hence we have $\Delta L \geq \sqrt{L}\,(SNR_{\text{threshold}}/C)$ for chemotaxis. Therefore, the minimum differences of ligand concentration for chemotaxis are proportional to the square root of L, $\Delta L_{\text{threshold}} \propto \sqrt{L}$.

We should note that Eq. 1 may have an additional noise derived from the fluctuation of the ligand concentration in extracellular solution, which can be given by

$$\frac{\sigma_{\text{R}}^2}{\overline{R^*}^2} = g_{\text{R}}\frac{1}{\overline{R^*}} + g_{\text{R}}^2\frac{1}{\pi D\tau_{\text{R}}\bar{L}\phi}, \tag{12}$$

where D is the diffusion constant of the ligand and Φ is the cell size (23,43). Using $D \approx 10^3\ \mu\text{m}^2/\text{s}$ for cAMP and the other parameter values shown in Table 1 we find $\pi D\tau_{\text{R}}\bar{L}\phi \approx 50\overline{R^*} \gg \overline{R^*}$, indicating that the second term in Eq. 12, which is derived from the ligand concentration fluctuation in extracellular solution, is negligible.

We thank Paul R. Fisher for permission to use the experimental data reported in his published work (14) and Peter J. M. Van Haastert for valuable comments on his experimental data and our model. We also thank Toshio Yanagida for continuous encouragement and Peter Karagiannis for critical reading of the manuscript.

This study was supported by Leading Project of the Ministry of Education, Cultures, Sports, Science and Technology (MEXT), Japan.

REFERENCES

1. Ishijima, A., and T. Yanagida. 2001. Single molecule nanobioscience. *Trends Biochem. Sci.* 26:438–444.
2. Sako, Y., and T. Yanagida. 2003. Single-molecule visualization in cell biology. *Nat. Rev. Mol. Cell Biol.* 4:SS1–SS5.
3. Sakmann, B., and E. Neher. 1995. Single Channel Recording. Plenum, New York.
4. Funatsu, T., Y. Harada, M. Tokunaga, K. Saito, and T. Yanagida. 1995. Imaging of single fluorescent molecules and individual ATP turnovers by single myosin molecules in aqueous solution. *Nature*. 374:555–559.
5. Lu, H. P., L. Xun, and X. S. Xie. 1998. Single-molecule enzymatic dynamics. *Science*. 282:1877–1882.
6. Kitamura, K., M. Tokunaga, A. H. Iwane, and T. Yanagida. 1999. A single myosin head moves along an actin filament with regular steps of ~5.3 nm. *Nature*. 397:129–134.
7. Kinosita, K., Jr., K. Adachi, and H. Itoh. 2004. Rotation of F1-ATPase: how an ATP-driven molecular machine may work. *Annu. Rev. Biophys. Biomol. Struct.* 33:245–268.
8. Zigmond, S. H. 1974. Mechanisms of sensing chemical gradients by polymorphonuclear leukocytes. *Nature*. 249:450–452.
9. Devreotes, P. N., and S. H. Zigmond. 1988. Chemotaxis in eukaryotic cells: a focus on leukocytes and *Dictyostelium*. *Annu. Rev. Cell Biol.* 4:649–686.
10. Parent, C. A., and P. N. Devreotes. 1999. A cell's sense of direction. *Science*. 284:765–770.
11. Parent, C. A. 2004. Making all the right moves: chemotaxis in neutrophils and *Dictyostelium*. *Curr. Opin. Cell Biol.* 16:4–13.
12. Van Haastert, P. J., and P. N. Devreotes. 2004. Chemotaxis: signalling the way forward. *Nat. Rev. Mol. Cell Biol.* 5:626–634.
13. Mato, J. M., A. Losada, V. Nanjundiah, and T. M. Konijn. 1975. Signal input for a chemotactic response in the cellular slime mold *Dictyostelium discoideum*. *Proc. Natl. Acad. Sci. USA*. 72:4991–4993.
14. Fisher, P. R., R. Merkl, and G. Gerisch. 1989. Quantitative analysis of cell motility and chemotaxis in *Dictyostelium discoideum* by using an image processing system and a novel chemotaxis chamber providing stationary chemical gradients. *J. Cell Biol.* 108:973–984.
15. Van Haastert, P. J. M. 1997. Transduction of the chemotactic cAMP signal across the plasma membrane. *In* Dictyostelium. Y. Maeda, K. Inouye, and I. Takeuchi, editors. Universal Adacemy Press, Tokyo. 173–191.
16. Janssens, P. M. W., and P. J. M. Van Haastert. 1987. Molecular basis of transmembrane signal transduction in *Dictyostelium discoideum*. *Microbiol. Rev.* 51:396–418.
17. Johnson, R. L., R. Gundersen, D. Hereld, G. S. Pitt, S. Tugendreich, C. L. Saxe, A. R. Kimmel, and P. N. Devreotes. 1992. G-protein-linked signaling pathways mediate development in *Dictyostelium*. *Cold Spring Harb. Symp. Quant. Biol.* 57:169–176.
18. Song, L., S. M. Nadkarni, H. U. Bödeker, C. Beta, A. Bae, C. Franck, W.-J. Rappel, W. F. Loomis, and E. Bodenschatz. 2006. *Dictyostelium discoideum* chemotaxis: threshold for directed motion. *Eur. J. Cell Biol.* 85:981–989.
19. Ueda, M., Y. Sako, T. Tanaka, P. Devreotes, and T. Yanagida. 2001. Single-molecule analysis of chemotactic signaling in *Dictyostelium* cells. *Science*. 294:864–867.
20. Oosawa, F. 1975. The effect of field fluctuation on a macromolecular system. *J. Theor. Biol.* 25:175–186.
21. Oosawa, F. 1990. Hierarchy of noise production in living cells. *In* White Noise Analysis. H. Hida, H. H. Kuo, J. Potthoff, and L. Streit, editors. World Scientific, Singapore. 315–329.
22. Oosawa, F. 2001. Spontaneous signal generation in living cells. *Bull. Math. Biol.* 63:643–654.
23. Berg, H. C., and E. M. Purcell. 1977. Physics of chemoreception. *Biophys. J.* 20:193–219.
24. Tranquillo, R. T., D. A. Lauffenburger, and S. H. Zigmond. 1988. A stochastic model for leukocyte random motility and chemotaxis based on receptor binding fluctuations. *J. Cell Biol.* 106:303–309.
25. Tranquillo, R. T. 1990. Theories and models of gradient perception. *In* Biology of the Chemotactic Response. J. P. Armitage and J. M. Lackie, editors. Cambridge University Press, Cambridge, UK. 35–75.
26. Elowitz, M. B., A. J. Levine, E. D. Siggia, and P. S. Swain. 2002. Stochastic gene expression in a single cell. *Science*. 297:1183–1186.
27. Rosenfeld, N., J. W. Young, U. Alon, P. S. Swain, and M. B. Elowitz. 2005. Gene regulation at the single-cell level. *Science*. 307:1962–1965.
28. Pedraza, J. M., and A. van Oudenaarden. 2005. Noise propagation in gene networks. *Science*. 307:1965–1969.
29. Hooshangi, S., S. Thiberge, and R. Weiss. 2005. Ultrasensitivity and noise propagation in a synthetic transcriptional cascade. *Proc. Natl. Acad. Sci. USA*. 102:3581–3586.
30. Paulsson, J. 2004. Summing up the noise in gene networks. *Nature*. 427:415–418.
31. Shibata, T., and K. Fujimoto. 2005. Noisy signal amplification in ultrasensitive signal transduction. *Proc. Natl. Acad. Sci. USA*. 102: 331–336.
32. Ueda, M., Y. Miyanaga, and T. Yanagida. 2005. Single-molecule analysis of chemotactic signaling mediated by cAMP receptor on living cells. *In* Methods in Signal Transduction, Series 6. T. Haga, and S. Takeda, editors. CRC Press, Boca Raton, FL. 197–218.
33. Gerisch, G., D. Hulser, D. Malchow, and U. Wick. 1975. Cell communication by periodic cyclic-AMP pulses. *Philos. Trans. R. Soc. Lond. B Biol. Sci.* 272:181–192.
34. Kutscher, B., P. N. Devreotes, and P. A. Iglesias. 2004. Local excitation, global inhibition mechanism for gradient sensing: an interactive applet. *Sci. STKE*. 2004:l3.
35. Ma, L., C. Janetopoulos, L. Yang, P. N. Devreotes, and P. A. Iglesias. 2004. Two complementary, local excitation, global inhibition mechanisms acting in parallel can explain the chemoattractant-induced regulation of PI(3,4,5)P3 response in *Dictyostelium* cells. *Biophys. J.* 87:3764–3774.
36. Janetopoulos, C., T. Jin, and P. Devreotes. 2001. Receptor-mediated activation of heterotrimeric G-proteins in living cells. *Science*. 291: 2408–2411.

37. Zigmond, S. H. 1977. Ability of polymorphonuclear leukocytes to orient in gradients of chemotactic factors. *J. Cell Biol.* 75:606–616.

38. Rosoff, W. J., J. S. Urbach, M. A. Esrick, R. G. McAllister, L. J. Richards, and G. J. Goodhill. 2004. A new chemotaxis assay shows the extreme sensitivity of axons to molecular gradients. *Nat. Neurosci.* 7: 678–682.

39. Van Haastert, P. J. 1983. Sensory adaptation of *Dictyostelium discoideum* cells to chemotactic signals. *J. Cell Biol.* 96:1559–1565.

40. Swanson, J. A., and D. L. Taylor. 1982. Local and spatially coordinated movements in *Dictyostelium discoideum* amoebae during chemotaxis. *Cell.* 28:225–232.

41. Xiao, Z., Y. Yao, Y. Long, and P. N. Devreotes. 1999. Desensitization of G-protein-coupled receptors. agonist-induced phosphorylation of the chemoattractant receptor cAR1 lowers its intrinsic affinity for cAMP. *J. Biol. Chem.* 274:1440–1448.

42. Postma, M., J. Roelofs, J. Goedhart, H. M. Loovers, A. J. Visser, and P. J. Van Haastert. 2004. Sensitization of *Dictyostelium* chemotaxis by phosphoinositide-3-kinase-mediated self-organizing signalling patches. *J. Cell Sci.* 117:2925–2935.

43. Bialek, W., and S. Setayeshgar. 2005. Physical limits to biochemical signaling. *Proc. Natl. Acad. Sci. USA.* 102:10040–10045.

44. Gillespie, D. T. 1977. Exact stochastic simulation of coupled chemical-reactions. *J. Phys. Chem.* 81:2340–2361.